ARTICLE

doi:10.1038/nature21365

Adipose-derived circulating miRNAs regulate gene expression in other tissues

Thomas Thomou[1], Marcelo A. Mori[2], Jonathan M. Dreyfuss[3,4], Masahiro Konishi[1], Masaji Sakaguchi[1], Christian Wolfrum[5], Tata Nageswara Rao[1,6], Jonathon N. Winnay[1], Ruben Garcia-Martin[1], Steven K. Grinspoon[7], Phillip Gorden[8] & C. Ronald Kahn[1]

Adipose tissue is a major site of energy storage and has a role in the regulation of metabolism through the release of adipokines. Here we show that mice with an adipose-tissue-specific knockout of the microRNA (miRNA)-processing enzyme Dicer (ADicerKO), as well as humans with lipodystrophy, exhibit a substantial decrease in levels of circulating exosomal miRNAs. Transplantation of both white and brown adipose tissue—brown especially—into ADicerKO mice restores the level of numerous circulating miRNAs that are associated with an improvement in glucose tolerance and a reduction in hepatic *Fgf21* mRNA and circulating FGF21. This gene regulation can be mimicked by the administration of normal, but not ADicerKO, serum exosomes. Expression of a human-specific miRNA in the brown adipose tissue of one mouse *in vivo* can also regulate its 3′ UTR reporter in the liver of another mouse through serum exosomal transfer. Thus, adipose tissue constitutes an important source of circulating exosomal miRNAs, which can regulate gene expression in distant tissues and thereby serve as a previously undescribed form of adipokine.

MicroRNAs are 19–22-nucleotide-long non-coding RNAs that function as negative regulators of translation and are involved in many cellular processes[1–5]. Many miRNAs exist in the circulation as well as in tissues[6], and a large fraction of these are found in exosomes[7] (50–200-nm vesicles that are released from multivesicular bodies[8]). Increased levels of specific miRNAs have been associated with a variety of diseases, including cancer[9], diabetes[3,10,11] obesity[12], and cardiovascular disease[13]. miRNAs have an important role in the differentiation and function of many cells, including those in adipose tissue[14]. The amount of white adipose tissue (WAT) miRNAs declines with age, owing to a decrease in the miRNA-processing enzyme Dicer[15], and similar decreases are also observed in humans with HIV-associated lipodystrophy[16] for the same reason. To understand more clearly the role of miRNAs in fat, we generated mice specifically lacking Dicer in adipose tissue using a Cre-*lox* gene-recombination strategy[15] (Fig. 1a). ADicerKO mice exhibited a defect in miRNA processing in adipose tissue, resulting in a decrease in WAT, the whitening of brown adipose tissue (BAT), insulin resistance and alterations to circulating lipids[16].

Adipose tissue is a major source of circulating miRNAs

To determine the extent to which adipose tissue contributes to circulating miRNAs, we isolated exosomes from the serum of 6-month-old male ADicerKO and wild-type control mice by differential ultracentrifugation[17]. These vesicles were 80–200 nm in diameter[18] (Extended Data Fig. 1a) and positively stained for the exosomal markers CD63 and CD9 (refs 19, 20) (Fig. 1b). The number of exosomes isolated from ADicerKO and control mice was comparable (Extended Data Fig. 1b, c). Quantitative PCR with reverse transcription (qRT–PCR) profiling of serum exosomes for 709 mouse miRNAs revealed 653 detectable miRNAs (defined as those with threshold cycle (C_t) below 34). ADicerKO mice exhibited significant ($P < 0.05$, R/Bioconductor limma package; see Methods) alterations in 422 exosomal miRNAs compared to control mice. Of these, three miRNAs were significantly increased, whereas 419 were significantly decreased (Fig. 1c, d, Extended Data Fig. 1d and Supplementary Table 1), with 88% reduced by more than fourfold, suggesting that adipose tissue is a major source of circulating exosomal miRNAs. Consistent with this finding, many of the miRNAs that were depleted in ADicerKO samples (Supplementary Table 1), including miR-221, miR-201, miR-222 and miR-16, have been shown to be highly expressed in fat[11,21–23].

miRNAs also exist in the circulation outside of exosomes. In a set of 80 miRNAs, there was a broad reduction in total miRNAs in the serum of ADicerKO mice when compared to the wild type (Extended Data Fig. 2a); however, this reduction was not as marked as the reduction in exosomal miRNAs, indicating that adipose tissue makes a particular contribution to the exosomal miRNA fraction. The loss of exosomal miRNA secretion in adipocytes lacking Dicer is cell-autonomous. Thus, in pre-adipocytes isolated from *Dicer*$^{fl/fl}$ mice and then transduced with Ad-Cre adenovirus *in vitro*, the levels of most of the detectable miRNAs (of the 380 miRNAs profiled) released in exosomes into the medium were decreased when compared to levels in Ad-GFP-transfected (control) cells (Extended Data Fig. 2b).

To further dissociate altered metabolism from lipodystrophy as a cause of reduced exosomal miRNAs, we compared serum miRNAs from 4-week-old control and ADicerKO mice, since, at this age, the metabolic phenotypes of ADicerKO mice are similar to those of wild-type mice (Extended Data Fig. 2c). Of the 380 miRNAs profiled, 373 were detectable, with 202 downregulated and only 23 upregulated in ADicerKO mice, indicating that the reduction in circulating exosomal miRNAs primarily reflects differences in miRNA processing and production rather than the effects of chronic lipodystrophy.

To investigate whether circulating miRNAs in humans also originate from fat, we performed exosomal miRNA profiling on the serum of patients with congenital generalized lipodystrophy (CGL) and patients with HIV-associated lipodystrophy; the former have a generalized loss of adipose tissue and the latter have previously

[1]Section on Integrative Physiology & Metabolism, Joslin Diabetes Center and Harvard Medical School, Boston, Massachusetts, USA. [2]Department of Biochemistry and Tissue Biology, University of Campinas, Campinas, Brazil. [3]Bioinformatics Core, Joslin Diabetes Center and Harvard Medical School, Boston, Massachusetts, USA. [4]Department of Biomedical Engineering, Boston University, Boston, Massachusetts, USA. [5]ETHZ, Department of Health Sciences and Metabolism, Zurich, Switzerland. [6]Department of Biomedicine, Experimental Hematology, University Hospital Basel, Switzerland. [7]MGH Program in Nutritional Metabolism, Massachusetts General Hospital and Harvard Medical School, Boston, Massachusetts, USA. [8]Diabetes, Endocrinology and Obesity Branch, NIDDK, National Institutes of Health, Bethesda, Maryland, USA.

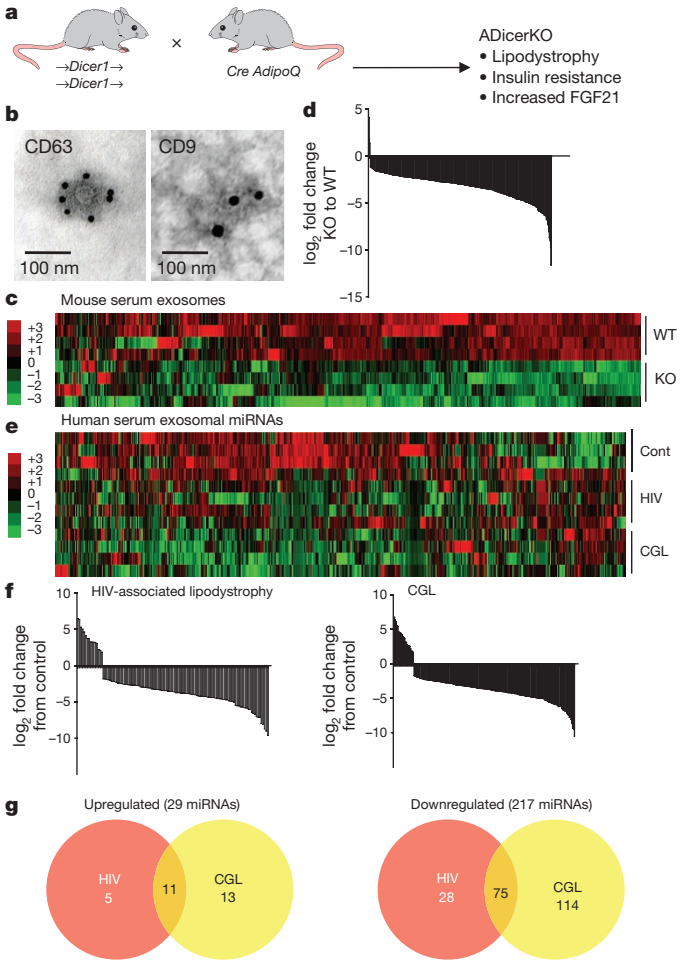

Figure 1 | Fat tissue is a major source of exosomal miRNAs. a, Schematic showing the creation of ADicerKO mice. **b**, Immuno-electron micrographs of CD63 and CD9 in mouse serum exosomes. **c**, Heatmap showing *Z* scores of exosomal miRNAs from the serum of ADicerKO mice and Lox (wild type; WT) littermates ($n = 4$ per group). **d**, Waterfall plot showing the difference in the relative abundance of exosomal miRNAs in serum from ADicerKO and control mice. $P < 0.05$ ($n = 4$ per group). **e**, Heatmap showing *Z* scores of exosomal miRNAs in serum from humans with HIV-associated lipodystrophy (HIV), CGL and controls ($n = 4$ per group). **f**, Waterfall plots representing the relative abundance of exosomal miRNAs that were expressed differentially among HIV-associated lipodystrophy, CGL and controls ($n = 4$ per group, $P < 0.05$). **g**, Venn diagrams representing miRNAs that were significantly up- or downregulated in serum from patients with HIV or CGL compared to control serum. $P < 0.05$ ($n = 4$ per group; R/Bioconductor limma package, see Methods).

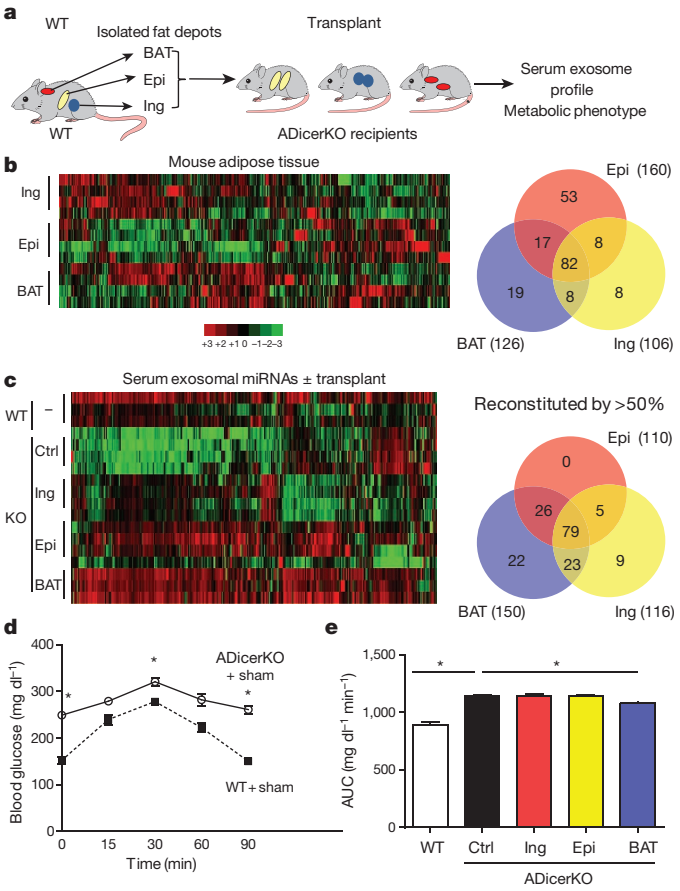

Figure 2 | Fat depot contributions to circulating exosomal miRNAs. **a**, Schematic of fat transplantation experiment using wild-type donor fat depots transplanted into ADicerKO recipients. **b**, Heatmap showing *Z* scores of miRNA expression in inguinal (Ing), epididymal (Epi) and brown adipose tissue (BAT) from wild-type donor mice ($n = 4$ per group). The Venn diagram depicts the number of fat-depot-specific miRNAs with an expression level greater than the U6 snRNA in wild-type mice ($n = 4$ per group). **c**, Heatmap of *Z* scores of exosomal miRNAs in ADicerKO or wild-type mice after sham surgery (Ctrl and WT, respectively) or transplantation of fat (all others; $n = 4$ per group). The Venn diagram represents miRNAs whose expression was restored to at least 50% of the value for wild-type mice after transplantation. $P < 0.05$ ($n = 4$ per group; R/Bioconductor limma package, see Methods). **d**, Glucose tolerance test in wild-type and ADicerKO mice. $P = 0.0001$ at 0 min; $P = 0.013$ at 15 min; $P = 0.0001$ at 90 min, all by two-tailed *t*-test ($n = 3$ per group). **e**, Area under the curve of glucose tolerance tests in ADicerKO and wild-type mice after sham surgery (Ctrl and WT, respectively), and ADicerKO mice after transplantation with the indicated type of fat tissue. $P = 0.0002$, wild type versus ADicerKO; $P = 0.033$, ADicerKO versus ADicerKO transplanted with BAT by two-tailed *t*-test ($n = 3$ per group). Data are mean ± s.e.m. $^*P < 0.05$.

been shown to have decreased levels of Dicer in fat[16] (Extended Data Fig. 3a). Similar numbers of exosomes were isolated from control and lipodystrophic patients (Extended Data Fig. 3b). Profiling of 572 miRNAs in exosomes using qRT–PCR identified 119 that differed significantly ($P < 0.05$, R/Bioconductor limma package; see Methods) between control subjects and those with HIV-associated lipodystrophy and 213 that differed significantly between control subjects and those with CGL (Fig. 1e, f, Extended Data Fig. 3c and Supplementary Tables 2, 3). Of these, only 5% (29 miRNAs) were upregulated in subjects with CGL or HIV-associated lipodystrophy, whereas 217 (38%) were downregulated, 75 in both CGL and HIV-associated lipodystrophy (Fig. 1g and Supplementary Table 4). Again, several of these miRNAs have been previously implicated in the regulation of fat[11,12,22,24]. Thirty miRNAs that were decreased in serum of both patient cohorts were also decreased in the serum of ADicerKO mice (Supplementary Table 5).

Fat transplantation reconstitutes circulating miRNAs

To verify that adipose tissue is an important source of circulating miRNAs, we transplanted fat from normal mice into ADicerKO mice (Fig. 2a). MicroRNA profiling of subcutaneous inguinal WAT, intra-abdominal epididymal WAT and BAT from wild-type donor mice revealed distinct, depot-specific signatures, consistent with previous studies[25] (Fig. 2b, Extended Data Fig. 4a and Supplementary Table 6). We considered miRNAs that were expressed at greater levels than the U6 small nuclear RNA (snRNA) as being highly expressed. Using this criterion, we identified 126 miRNAs that were highly expressed in BAT, 106 in inguinal WAT, and 160 in epididymal WAT, with 82 miRNAs

being highly expressed in all three depots (Fig. 2b). During the following two weeks, all mice maintained a consistent body weight; at death, the transplanted fat weighed 80–90% of its original weight, indicating successful engraftment (Extended Data Fig. 4b, c). As in the cohort of mice shown in Fig. 1, levels of circulating exosomal miRNAs were markedly reduced in ADicerKO mice that underwent sham surgery when compared to wild-type mice (Fig. 2c). By comparison, ADicerKO mice that received fat transplants showed restoration of circulating exosomal miRNAs (Fig. 2c, Extended Data Fig. 5a and Supplementary Tables 7 and 8). Of the 177 circulating exosomal miRNAs that were detectable in the serum of wild-type mice and significantly decreased in that of ADicerKO mice, fat transplantation restored the levels of the majority to at least 50% of normal levels, indicating that adipose tissue is a major source of circulating exosomal miRNAs and that different depots contribute to different degrees.

Physiologically, ADicerKO mice had significantly impaired glucose tolerance compared to wild-type mice, with an approximate increase of 50% in the area under the curve (Fig. 2d, e). This improved only slightly after transplantation of inguinal WAT or epididymal WAT; however, glucose tolerance test results were significantly ($P < 0.05$, two-tailed *t*-test) improved in ADicerKO mice that received BAT transplants (Fig. 2e). ADicerKO mice also exhibit considerable insulin resistance, as indicated by increased circulating insulin levels; this resistance was also reduced in the group receiving BAT transplants, but the reduction did not reach statistical significance (Extended Data Fig. 5b). Levels of serum IL-6, leptin and adiponectin were all lower in ADicerKO mice than in control mice and were not restored by transplantation (Extended Data Fig. 5b).

Circulating exosomal miRNAs might regulate FGF21

Fibroblast growth factor 21 (FGF21) is produced in the liver and other tissues. On its release into the circulation, it influences metabolism in multiple tissues[26,27]. ADicerKO mice exhibited an approximately threefold increase in circulating FGF21, which was associated with increased levels of *Fgf21* mRNA in liver, muscle, fat and pancreas (Fig. 3a, b and Extended Data Fig. 6a). After transplantation of WAT, serum FGF21 and liver *Fgf21* mRNA levels remained unchanged in ADicerKO mice (Fig. 3c, d). However, levels of *Fgf21* mRNA in the livers of ADicerKO mice were reduced by approximately 50% after BAT transplantation (Fig. 3d). This occurred in parallel with a reduction in the amount of circulating FGF21 (Fig. 3c), indicating that BAT transplantation provided some factor(s) that directly or indirectly regulated FGF21 expression in the liver. Hypothesizing that one regulatory factor could be a circulating miRNA, we searched the miRDB database to identify miRNAs that might target the 3′ untranslated region (UTR) of mouse *Fgf21* mRNA[28]. Four candidates were identified (miR-99a, miR-99b, miR-100, and miR-466i), three of which (miR-99a, miR-99b, and miR-100) were significantly ($P < 0.05$, R/Bioconductor limma package; see Methods) decreased in the serum of ADicerKO mice compared to controls. Although these three miRNAs were restored to near wild-type levels in all ADicerKO transplanted mice, only ADicerKO mice that received BAT transplants exhibited expression levels higher than the wild type, which tracked with reductions in levels of circulating FGF21 (Extended Data Fig. 6b). To investigate which of these miRNAs might regulate FGF21, we transfected AML-12 liver cells with an adenoviral pacAd5-FGF21-3′-UTR-luciferase reporter and, after 2 days, transfected the cells with 10 nM of a candidate or control miRNA mimic. Of these, only transfection with miR-99b resulted in a robust reduction in FGF21–luciferase activity (Extended Data Fig. 7a), correlating with a 65% reduction in *Fgf21* mRNA (Extended Data Fig. 7b).

To test whether these miRNAs could regulate FGF21 expression when presented in exosomes, we exposed AML-12 cells expressing the *Fgf21* 3′ UTR–luciferase reporter to exosomes from wild-type or ADicerKO mice, or to ADicerKO exosomes that had been electroporated with miR-99a, miR-99b, miR-100, miR-466i or a control mimic. We found that the isolated exosomes from control mice could suppress *Fgf21* 3′ UTR–luciferase activity by 60% *in vitro*, whereas exosomes from the serum of ADicerKO mice had no effect (Fig. 3e). Furthermore, while treatment with exosomes from ADicerKO mice reconstituted with miR-99a, miR-100 or miR-466i had minimal effects, exosomes bearing miR-99b resulted in a reduction of luciferase activity of approximately 55% (Fig. 3f) along with an equal reduction in *Fgf21* mRNA levels, mimicking the effects of wild-type exosomes (Extended Data Fig. 7c). This regulation of FGF21 was dependent on exosomal delivery and was not recapitulated when cells were incubated with naked miR-99b (Fig. 3e).

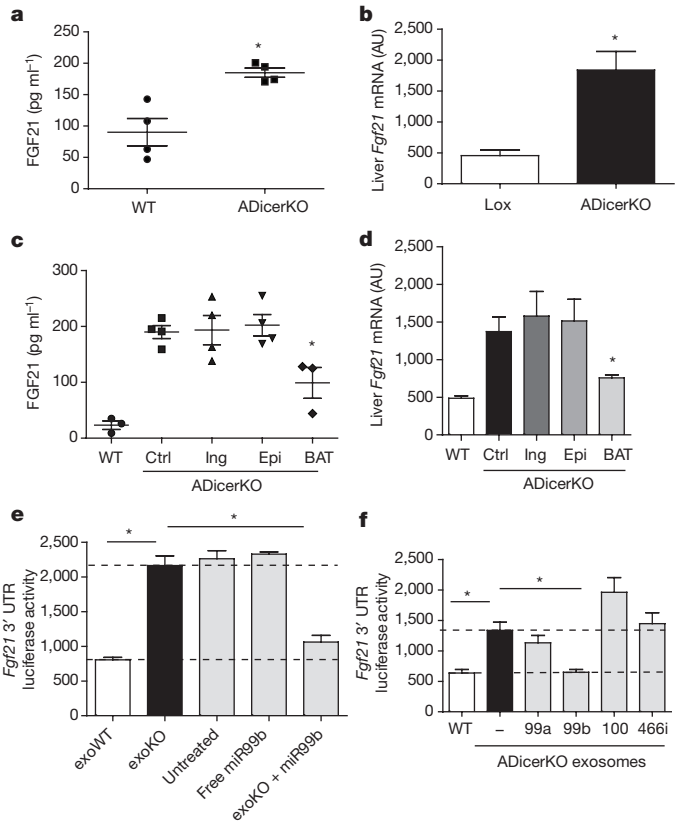

Figure 3 | Fat-derived exosomal miRNAs regulate hepatic FGF21 and transcription. a, Enzyme-linked immunosorbant assay (ELISA), measuring the amount of FGF21 in the serum of ADicerKO and wild-type littermates. $P = 0.028$ by two-tailed Mann–Whitney *U*-test ($n = 4$ per group). **b**, qRT–PCR of hepatic *Fgf21* mRNA in ADicerKO mice and Lox littermates. $P = 0.028$ by two-tailed Mann–Whitney *U*-test ($n = 4$ per group). **c**, Serum levels of FGF21 in ADicerKO mice that underwent sham surgery (Ctrl), wild-type mice that underwent sham surgery (WT) and ADicerKO mice transplanted with the indicated type of adipose tissue. $P = 0.019$, wild-type versus ADicerKO transplanted with BAT by two-tailed *t*-test ($n = 3$ per group). **d**, qRT–PCR of hepatic *Fgf21* mRNA of the same mice as in **c**. $P = 0.046$, ADicerKO sham versus ADicerKO transplanted with BAT by two-tailed *t*-test ($n = 3$ per group). **e**, *Fgf21* 3′ UTR luciferase activity after incubation of AML-12 cells with exosomes from Lox (exoWT) or ADicerKO (exoADicerKO) mice, 10 nM free miR-99b or exosomes derived from ADicerKO mice electroporated with miR-99b (exoADicerKO + miR-99b). $P = 0.008$, wild-type exosomes versus ADicerKO exosomes; $P = 0.008$, ADicerKO exosomes versus ADicerKO with miR-99b by two-tailed *t*-test ($n = 3$ per group). **f**, *Fgf21* 3′ UTR luciferase activity following the incubation of AML-12 cells with exosomes from ADicerKO mice (−), Lox littermates, or from ADicerKO mice that had been electroporated to introduce miR-99a, miR-99b, miR-100 or miR-466i. $P = 0.0007$, exosomes from wild-type versus untreated ADicerKO mice; $P = 0.002$, exosomes from untreated ADicerKO versus ADicerKO mice electroporated with miR-99b by two-tailed *t*-test ($n = 3$ per group). AU, arbitrary units. $^*P < 0.05$.

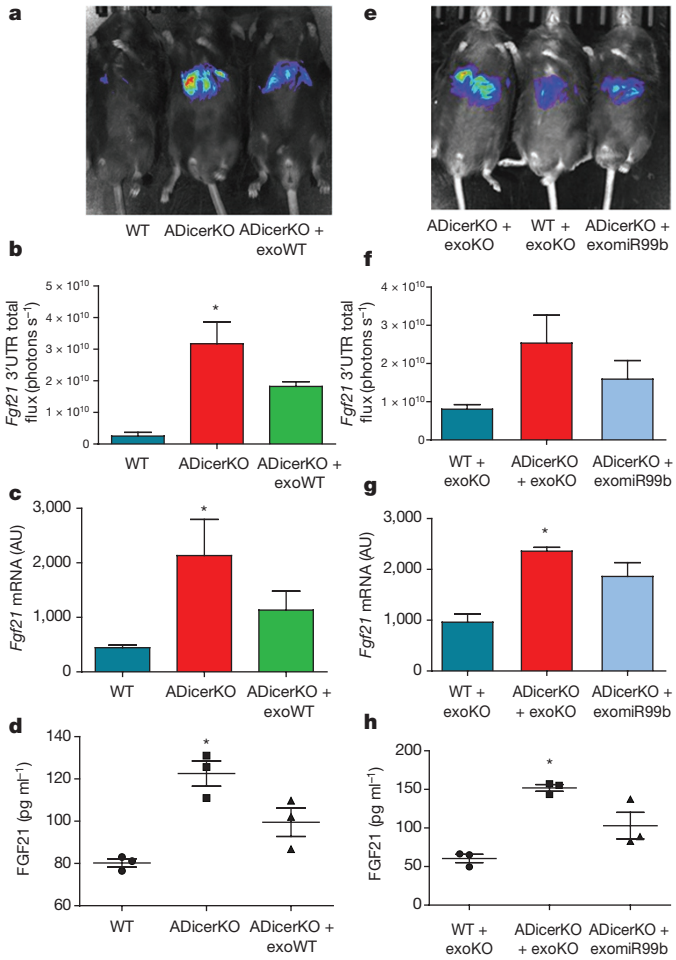

Figure 4 | *In vivo* regulation of FGF21 via exosomal miR-99b. a, Lox, ADicerKO, and ADicerKO mice injected intravenously with exosomes from wild-type mice (ADicerKO + exoWT) transfected with the pacAd5-Luc-FGF21-3′UTR-luciferase reporter and subjected to IVIS analysis. **b**, Total flux luminescence of the mice in **a**, as measured by IVIS. $P = 0.039$, wild-type versus ADicerKO mice. **c**, qRT–PCR of hepatic *Fgf21* mRNA in above mice. $P = 0.039$, wild-type versus ADicerKO mice. **d**, ELISA measuring FGF21 concentration in serum from the above mice. $P = 0.027$, wild-type versus ADicerKO mice. **e**, Lox mice injected intravenously with ADicerKO exosomes (WT + exoADicerKO) and ADicerKO mice injected with either ADicerKO exosomes (ADicerKO + exoADicerKO) or ADicerKO exosomes electroporated with miR-99b (ADicerKO + exomiR99b), subjected to IVIS analysis. **f**, Total flux luminescence in IVIS from mice in **e**; $P = 0.079$. **g**, qRT–PCR of hepatic *Fgf21* mRNA of mice in **e**. $P = 0.039$, wild-type mice injected with ADicerKO exosomes versus ADicerKO mice injected with ADicerKO exosomes. **h**, ELISA of serum FGF21 of mice in **e**. $P = 0.027$, wild-type mice injected with ADicerKO exosomes versus ADicerKO mice injected with ADicerKO exosomes ($n = 3$ per group). Note that the order of the data in **f**–**h** is different from the order of the mice shown in **e**, because the IVIS scan was done in a blinded fashion. Data are mean ± s.e.m. *P* values in **b**–**d**, **f**–**h** obtained by Kruskal–Wallis analysis of variance (ANOVA) with Dunn's post-hoc test; $n = 3$; $^*P < 0.05$.

To investigate the regulation of *Fgf21* mRNA by exosomal miRNAs *in vivo*, we transfected ADicerKO and wild-type mice with a pacAd5-FGF21-3′-UTR-luciferase reporter and measured the suppression of hepatic FGF21 expression using the IVIS *in vivo* imaging system. Consistent with the data obtained *in vitro*, *Fgf21* 3′ UTR activity *in vivo* was fivefold higher in ADicerKO mice than in wild-type mice, reflecting the absence of repressive circulating miRNAs in ADicerKO mice (Fig. 4a, b). Injection of wild-type exosomes into ADicerKO mice suppressed the elevated FGF21 reporter activity by around 60%. This was confirmed by qRT–PCR, which showed that there was a reduction in elevated hepatic *Fgf21* mRNA and a parallel decrease in circulating FGF21 compared to untreated ADicerKO mice (Fig. 4c, d). Consistent with the idea that BAT-secreted exosomes deliver miRNAs to the liver, levels of miR-16, miR-201 and miR-222, which are relatively fat-specific, were significantly ($P < 0.05$, one-way ANOVA, Tukey's multiple comparisons test) decreased in the livers of ADicerKO mice and restored towards normal by BAT transplantation (Extended Data Fig. 8a). There was no change in the corresponding pre-miRNA species in the liver (Extended Data Fig. 8b).

In separate experiments, we injected wild-type and ADicerKO mice with exosomes from ADicerKO mice, with or without reconstitution of miR-99b (Fig. 4e). Again, ADicerKO mice showed 2.5-fold higher luciferase activity than wild-type mice when both were injected with exosomes from ADicerKO mice. Administration of ADicerKO exosomes reconstituted with miR-99b re-induced suppression of the *Fgf21* 3′ UTR reporter 45% of the way towards normal (Fig. 4f). This was accompanied by a parallel reduction in hepatic *Fgf21* mRNA (Fig. 4g) and in the amount of circulating FGF21 (Fig. 4h).

Regulation of liver gene expression by exosomal miRNAs

The regulation of FGF21 is a complex process that involves multiple factors. To assess the role of fat-derived circulating miRNAs *in vivo*, we developed a more specific reporter system, which took advantage of the human-specific miRNA hsa_miR-302f and its 3′ UTR reporter[29], as this miRNA does not have a mouse homologue. We then performed two types of experiment. In the first protocol (Protocol 1; Fig. 5a) we injected an adenovirus vector bearing either pre-hsa_miR-302f or a control sequence directly into BAT to induce BAT-specific expression of the transfected gene[30]. Three days later, we injected the same mice intravenously with an adenovirus bearing the 3′ UTR luciferase reporter for hsa_miR-302f to induce its expression in the liver. Suppression of the reporter would be observed only if there was communication between the miRNA expressed in the BAT and the reporter expressed in the liver. IVIS analysis 5 days after transduction revealed that there was a reduction of more than 95% in luciferase activity in the liver of mice transfected with miR-302f into their BAT when compared to mice with *lacZ*-transfected BAT (control) (Fig. 5b, c).

In the second protocol (Protocol 2; Fig. 5d), to address definitively whether hsa_miR-302f-mediated reporter suppression in liver tissue was contingent on exosomal delivery, we used two separate cohorts of C57BL/6 mice. The first cohort was transfected with an adenovirus bearing either pre-hsa_miR-302f or *lacZ* directly into the BAT (the donor cohort). The liver of the second, separate cohort of mice was transduced by intravenous injection of the adenovirus bearing the 3′ UTR hsa_miR-302f reporter (the acceptor cohort). We then obtained serum from the donor cohorts over the following 8 days, isolated the exosomes, injected the purified exosomes intravenously into the acceptor mice and performed IVIS analysis of the 3′ UTR hsa_miR-302f reporter. In comparison to the mice that received exosomes from the mice whose BAT was transfected with *lacZ*, acceptor mice that were injected with exosomes from donors whose BAT was transfected with hsa_miR-302f exhibited a 95% reduction in luciferase activity in the liver (Fig. 5e, f), demonstrating that this circulating exosomal miRNA, which is produced in the adipose tissue, regulates the activity of its reporter in the liver tissue of recipient mice. This result was not due to uptake by the liver of miR-302f adenovirus that might have leaked from BAT, since we detected no viral DNA expressing miR-302f (or *lacZ* in controls) in the livers of the animals used in either protocol, as assessed by qRT–PCR (Extended Data Fig. 8c; $C_t > 40$).

A new role for fat and its potential implications

Together, our data show that adipose tissue is an important source of circulating exosomal miRNAs in both mice and humans. Our data also demonstrate that circulating exosomal miRNAs derived from fat may regulate whole-body metabolism and mRNA translation in

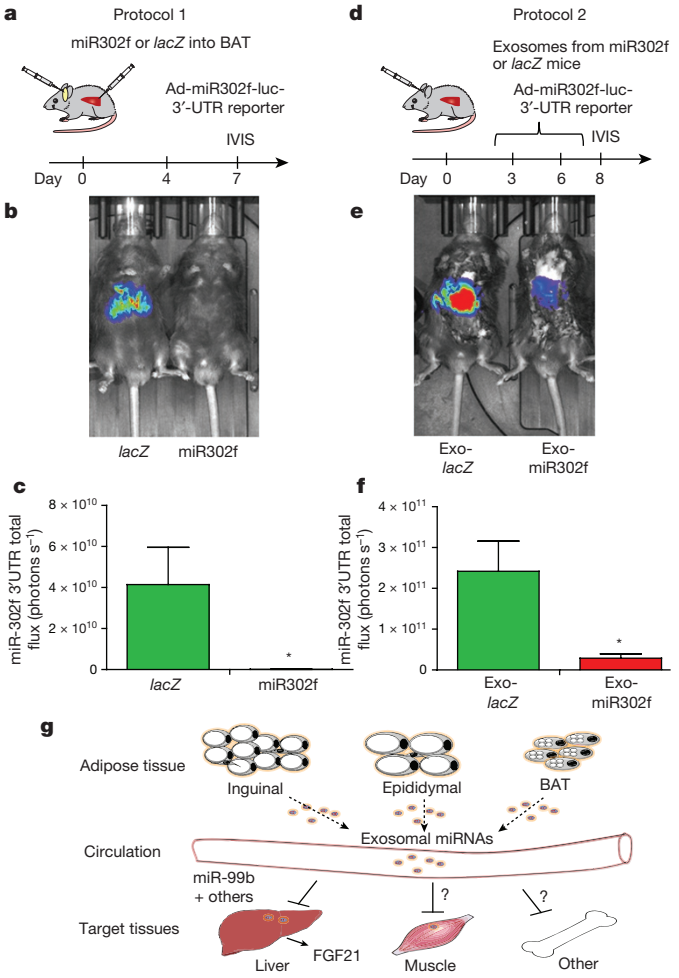

Figure 5 | BAT-derived exosomes expressing human miRNA miR-302f target their reporter in liver *in vivo*. **a**, Schematic of Protocol 1, the *in vivo* targeting protocol that used adenovirus bearing pre-miR-302f or *lacZ* directly into BAT. **b**, Wild-type mice injected intravenously with the pacAd5-hsa_miR-302f 3′ UTR reporter after injection of Ad-pre-hsa-miR-302f or Ad-lacZ into the BAT and subjected to IVIS ($n = 4$ per group). **c**, Total flux luminescence obtained via IVIS analysis from mice in **b**; $P = 0.028$. **d**, Schematic of Protocol 2, the *in vivo* targeting protocol in which exosomes from wild-type mice complemented with either pre-miR-302f or adenovirus bearing *lacZ* directly into was transfected into BAT. **e**, IVIS image of wild-type mice transfected with the pacAd5-hsa_miR-302f 3′ UTR reporter after intravenous injections of serum exosomes from mice whose BAT was injected with either Ad-pre-hsa_miR-302f or Ad-lacZ ($n = 4$ per group). **f**, Total flux luminescence obtained using the same protocol as in **e**; $P = 0.028$. Data are mean ± s.e.m. **g**, Model of mechanisms by which fat-derived circulating exosomal miRNAs might regulate target mRNAs in other tissues. *P* values in **c**, **f** obtained using Mann–Whitney *U*-test; $n = 4$. $^*P < 0.05$.

other tissues. Thus, adipose tissue transplantation, especially BAT transplantation, improves glucose tolerance and lowers levels of circulating insulin and FGF21, as well as hepatic *Fgf21* mRNA in recipient mice. The latter effect appears to be due, at least in part, to the direct effect of the circulating miRNAs on *Fgf21* expression in the liver, as incubation of exosomes from control mice with liver cells *in vitro* can lower *Fgf21* mRNA levels and repress the activity of an *Fgf21* 3′ UTR reporter. Exosomes isolated from ADicerKO mice do not induce this effect, but it can be reconstituted by the introduction of miR-99b, a predicted regulator of mouse FGF21. miR-99b is also one of the miRNAs that is strongly reduced in circulating exosomes from ADicerKO mice, and whose level is largely restored by BAT transplantation. Transplantation with WAT also significantly ($P < 0.05$, R/Bioconductor limma package; see Methods) restored the level of miR-99b in circulating exosomes, but only transplantation with BAT reduced hepatic *Fgf21* mRNA, suggesting that BAT-derived exosomes may target the liver more efficiently than WAT-derived exosomes. Such tissue-specific targeting has been suggested by previous *in vitro* studies[20,31], implying that inter-organ exosomal delivery is tissue-specific[32]. The generalizability of this type of cross-talk between adipose tissue and liver mRNA regulation is made ever clearer by the use of a human-specific miRNA reporter. Hence, when mouse BAT is transfected with an adenovirus that bears the human-specific miRNA hsa_miR-302f, exosomes present in the circulation of the mouse can target an hsa_miR-302f 3′ UTR reporter present in the liver of the same mouse or even a different mouse that has been injected with isolated exosomes from the appropriate donor.

As adipose tissue is an important source of circulating miRNAs, the loss of adipose-derived miRNAs in lipodystrophy and their restoration by fat transplantation may involve many more targets and tissues than just hepatic FGF21. miRNAs that are restored upon transplantation of BAT include miR-325 and miR-743b (predicted to target UCP-1 expression) and miR-98 (predicted to target PGC1α expression), suggesting that miRNAs secreted by adipose tissue may act at both the paracrine and endocrine levels. This finding could contribute to other aspects of the phenotype of ADicerKO mice, including features of metabolic syndrome and the 'whitening' of interscapular BAT[16]. The regulation of metabolism and mRNA expression in lipodystrophy could also involve other exosomal factors that are secreted into circulation by adipose tissue as well as a range of non-exosomal mechanisms, including conventional adipokines and cytokines, hormones and metabolic intermediates[33]. This study makes clear that, in addition to serving as markers of disease, exosomal miRNAs can be exported to other tissues, in which they also serve a regulatory role[34–38]. *In vitro*, endothelial exosomes have been shown to target vascular cells, providing protection from apoptosis[39]. Similarly, exosomes from mast cells can trigger other mast cells *in vitro*[32], whereas exosomes secreted by macrophages and/or platelets can be taken up by monocytes[35–38]. The exosomal transfer of miRNAs has been also reported in glioblastoma[17,40] and between embryonic stem cells and embryonic fibroblasts[41]. Although the majority of miRNAs present in the serum are contained within exosomes[42], adipose tissue could also contribute to circulating miRNAs through secretion in microvesicles or associated with Argonaute[43] or high-density lipoprotein[44]. The extent to which these forms of circulating miRNAs can regulate gene expression in distant tissues remains to be determined.

In summary, our data show that adipose tissue is an important source of circulating exosomal miRNAs and that different adipose depots contribute different exosomal miRNAs to the circulation. Our data also show that these adipose-derived circulating miRNAs can have far-reaching systemic effects, including on the regulation of mRNA expression and translation (Fig. 5g). As these miRNAs are produced by different adipose depots, their levels could also change in diseases with altered fat mass, such as lipodystrophy and obesity, or altered adipose distribution and function, such as diabetes and ageing. Thus, adipose-derived exosomal miRNAs constitute a previously undescribed class of adipokines that can act as regulators of metabolism in distant tissues, providing a new mechanism of cell–cell crosstalk.

Online Content Methods, along with any additional Extended Data display items and Source Data, are available in the online version of the paper; references unique to these sections appear only in the online paper.

Received 27 May 2016; accepted 4 January 2017.
Published online 15 February 2017.

1. Krol, J., Loedige, I. & Filipowicz, W. The widespread regulation of microRNA biogenesis, function and decay. *Nat. Rev. Genet.* **11,** 597–610 (2010).
2. Sun, L. *et al.* Mir193b-365 is essential for brown fat differentiation. *Nat. Cell Biol.* **13,** 958–965 (2011).

3. Trajkovski, M. *et al.* MicroRNAs 103 and 107 regulate insulin sensitivity. *Nature* **474,** 649–653 (2011).
4. Bartel, D. P. MicroRNAs: target recognition and regulatory functions. *Cell* **136,** 215–233 (2009).
5. Ameres, S. L. & Zamore, P. D. Diversifying microRNA sequence and function. *Nat. Rev. Mol. Cell Biol.* **14,** 475–488 (2013).
6. Arroyo, J. D. *et al.* Argonaute2 complexes carry a population of circulating microRNAs independent of vesicles in human plasma. *Proc. Natl Acad. Sci. USA* **108,** 5003–5008 (2011).
7. Thery, C., Amigorena, S., Raposo, G. & Clayton, A. *Curr Protoc Cell Biol* **Chapter 3,** Unit 3 22 (2006).
8. György, B. *et al.* Membrane vesicles, current state-of-the-art: emerging role of extracellular vesicles. *Cell. Mol. Life Sci.* **68,** 2667–2688 (2011).
9. Hata, A. & Lieberman, J. Dysregulation of microRNA biogenesis and gene silencing in cancer. *Sci. Signal.* **8,** re3 (2015).
10. Dumortier, O., Hinault, C. & Van Obberghen, E. MicroRNAs and metabolism crosstalk in energy homeostasis. *Cell Metab.* **18,** 312–324 (2013).
11. Arner, E. *et al.* Adipose tissue microRNAs as regulators of CCL2 production in human obesity. *Diabetes* **61,** 1986–1993 (2012).
12. Capobianco, V. *et al.* miRNA and protein expression profiles of visceral adipose tissue reveal miR-141/YWHAG and miR-520e/RAB11A as two potential miRNA/protein target pairs associated with severe obesity. *J. Proteome Res.* **11,** 3358–3369 (2012).
13. Caroli, A., Cardillo, M. T., Galea, R. & Biasucci, L. M. Potential therapeutic role of microRNAs in ischemic heart disease. *J. Cardiol.* **61,** 315–320 (2013).
14. Guay, C., Roggli, E., Nesca, V., Jacovetti, C. & Regazzi, R. Diabetes mellitus, a microRNA-related disease? Transl. *Res.* **157,** 253–264 (2011).
15. Mori, M. A. *et al.* Role of microRNA processing in adipose tissue in stress defense and longevity. *Cell Metab.* **16,** 336–347 (2012).
16. Mori, M. A. *et al.* Altered miRNA processing disrupts brown/white adipocyte determination and associates with lipodystrophy. *J. Clin. Invest.* **124,** 3339–3351 (2014).
17. Skog, J. *et al.* Glioblastoma microvesicles transport RNA and proteins that promote tumour growth and provide diagnostic biomarkers. *Nat. Cell Biol.* **10,** 1470–1476 (2008).
18. Taylor, D. D., Zacharias, W. & Gercel-Taylor, C. Exosome isolation for proteomic analyses and RNA profiling. *Methods Mol. Biol.* **728,** 235–246 (2011).
19. Escola, J. M. *et al.* Selective enrichment of tetraspan proteins on the internal vesicles of multivesicular endosomes and on exosomes secreted by human B-lymphocytes. *J. Biol. Chem.* **273,** 20121–20127 (1998).
20. Février, B. & Raposo, G. Exosomes: endosomal-derived vesicles shipping extracellular messages. *Curr. Opin. Cell Biol.* **16,** 415–421 (2004).
21. Ortega, F. J. *et al.* MiRNA expression profile of human subcutaneous adipose and during adipocyte differentiation. *PLoS One* **5,** e9022 (2010).
22. Chou, W. W. *et al.* Decreased microRNA-221 is associated with high levels of TNF-α in human adipose tissue-derived mesenchymal stem cells from obese woman. *Cell. Physiol. Biochem.* **32,** 127–137 (2013).
23. Oger, F. *et al.* Cell-specific dysregulation of microRNA expression in obese white adipose tissue. *J. Clin. Endocrinol. Metab.* **99,** 2821–2833 (2014).
24. Keller, P. *et al.* Gene-chip studies of adipogenesis-regulated microRNAs in mouse primary adipocytes and human obesity. *BMC Endocr. Disord.* **11,** 7 (2011).
25. McGregor, R. A. & Choi, M. S. microRNAs in the regulation of adipogenesis and obesity. *Curr. Mol. Med.* **11,** 304–316 (2011).
26. Potthoff, M. J., Kliewer, S. A. & Mangelsdorf, D. J. Endocrine fibroblast growth factors 15/19 and 21: from feast to famine. *Genes Dev.* **26,** 312–324 (2012).
27. Badman, M. K. *et al.* Hepatic fibroblast growth factor 21 is regulated by PPARalpha and is a key mediator of hepatic lipid metabolism in ketotic states. *Cell Metab.* **5,** 426–437 (2007).
28. Wong, N. & Wang, X. miRDB: an online resource for microRNA target prediction and functional annotations. *Nucleic Acids Res.* **43,** D146–D152 (2015).
29. Yao, Y. *et al.* MicroRNA profiling of human gastric cancer. *Mol. Med. Rep.* **2,** 963–970 (2009).
30. Uhrig-Schmidt, S. *et al.* Gene delivery to adipose tissue using transcriptionally targeted rAAV8 vectors. *PLoS One* **9,** e116288 (2014).
31. Atai, N. A. *et al.* Heparin blocks transfer of extracellular vesicles between donor and recipient cells. *J. Neurooncol.* **115,** 343–351 (2013).
32. Zech, D., Rana, S., Büchler, M. W. & Zöller, M. Tumor-exosomes and leukocyte activation: an ambivalent crosstalk. *Cell Commun. Signal.* **10,** 37 (2012).
33. Valadi, H. *et al.* Exosome-mediated transfer of mRNAs and microRNAs is a novel mechanism of genetic exchange between cells. *Nat. Cell Biol.* **9,** 654–659 (2007).
34. Blüher, M. Adipokines - removing road blocks to obesity and diabetes therapy. *Mol. Metab.* **3,** 230–240 (2014).
35. Théry, C., Ostrowski, M. & Segura, E. Membrane vesicles as conveyors of immune responses. *Nat. Rev. Immunol.* **9,** 581–593 (2009).
36. Bang, C. *et al.* Cardiac fibroblast-derived microRNA passenger strand-enriched exosomes mediate cardiomyocyte hypertrophy. *J. Clin. Invest.* **124,** 2136–2146 (2014).
37. Hergenreider, E. *et al.* Atheroprotective communication between endothelial cells and smooth muscle cells through miRNAs. *Nat. Cell Biol.* **14,** 249–256 (2012).
38. Mittelbrunn, M. *et al.* Unidirectional transfer of microRNA-loaded exosomes from T cells to antigen-presenting cells. *Nat. Commun.* **2,** 282 (2011).
39. Ismail, N. *et al.* Macrophage microvesicles induce macrophage differentiation and miR-223 transfer. *Blood* **121,** 984–995 (2013).
40. Zernecke, A. *et al.* Delivery of microRNA-126 by apoptotic bodies induces CXCL12-dependent vascular protection. *Sci. Signal.* **2,** ra81 (2009).
41. van der Vos, K. E. *et al.* Directly visualized glioblastoma-derived extracellular vesicles transfer RNA to microglia/macrophages in the brain. *Neuro-oncol.* **18,** 58–69 (2016).
42. Yuan, A. *et al.* Transfer of microRNAs by embryonic stem cell microvesicles. *PLoS One* **4,** e4722 (2009).
43. Gallo, A., Tandon, M., Alevizos, I. & Illei, G. G. The majority of microRNAs detectable in serum and saliva is concentrated in exosomes. *PLoS One* **7,** e30679 (2012).
44. Turchinovich, A., Weiz, L., Langheinz, A. & Burwinkel, B. Characterization of extracellular circulating microRNA. *Nucleic Acids Res.* **39,** 7223–7233 (2011).

Supplementary Information is available in the online version of the paper.

Acknowledgements We thank M. Torriani and K. V. Fitch for assistance with HIV lipodystrophy samples; M. Lynnes, S. Kasif, and A. M. Cypess for help with reagents and discussions; and the Joslin Histology, Media and Physiology Core Facilities for help with experiments. This study was supported by grants from the NIH R01 DK082659 and R01 DK033201, the Mary K. Iacocca Professorship, and the Joslin Diabetes Center DRC Grant P30DK036836. S.K.G. was funded by grants from the NIH (P30 DK040561). M.A.M. was funded by grants from FAPESP (2010/52557-0 and 2015/01316-7).

Author Contributions M.A.M. assisted with experimental design, generated the ADicerKO mice and designed the Ad-Luc-FGF2-3′-UTR constructs; J.M.D. carried out bioinformatics analysis; M.K. performed adenoviral injections in BAT; M.S. assisted with retro-orbital injections; C.W. created Ad-lacZ, Ad-pre-hsa-miR302f and Ad-Luc-miR302f-3′-UTR adenoviruses; T.N.R. assisted with retro-orbital and tail vain injections; J.N.W. assisted with fat depot miRNA PCR; R.G.-M. assisted with IVIS experiments and *in vitro* luminescence assays; S.K.G. provided human HIV lipodystrophy serum samples; P.G. provided human CGL sera samples; and T.T. and C.R.K. designed the study, collected and analysed data, and wrote the manuscript.

Author Information Reprints and permissions information is available at www.nature.com/reprints. The authors declare no competing financial interests. Readers are welcome to comment on the online version of the paper. Correspondence and requests for materials should be addressed to C.R.K. (c.ronald.kahn@joslin.harvard.edu).

METHODS

No statistical methods were used to predetermine sample size. The experiments were not randomized and the investigators were not blinded to allocation during experiments and outcome assessment. Animal experiments were neither randomized nor blinded. All animals used in this study (ADicerKO, Dicer$^{lox/lox}$, or C57BL/6) were males and 6 months of age unless specifically indicated otherwise. All animal experiments were conducted in accordance with IRB protocols with respect to live vertebrate experimentation. Human serum was obtained from human subjects after obtaining IRB approval and patients were given informed consent.

Exosome isolation, loading and immune-electron microscopy. Mouse and human sera were centrifuged at 1,000*g* for 5 min and then at 10,000*g* for 10 min to remove whole cells, cell debris and aggregates. The serum was subjected to 0.1-μm filtration and ultracentrifuged at 100,000*g* for 1 h. Pelleted vesicles were suspended in 1× PBS, ultracentrifuged again at 100,000*g* for washing, resuspended in 1× PBS and prepared for electron microscopy and immune-electron microscopy or miRNA extraction.

All *in vitro* experiments were carried out using exosome-free FBS. AML-12 cells were acquired from ATCC (cat no. CRL-2254) and were tested for mycoplasma contamination. *Dicer*$^{fl/fl}$ brown preadipocytes were generated as previously described[16]. For exosome loading, exosome preparations were isolated and diluted with PBS to final volume of 100 μl. Exosome electroporation was carried out by using a variation of a previously described technique[45]. Exosome preparations were mixed with 200 μl phosphate-buffered sucrose (272 mM sucrose 7 mM, K_2HPO_4) with 10 nM of a miRNA mimic, and the mixture was pulsed at 500 mV with 250 μF capacitance using a Bio-Rad Gene Pulser (Bio-Rad). Electroporated exosomes were resuspended in a total volume of 500 μl PBS and added to the target cells.

Isolated exosomes were subjected to immune-electron microscopy using standard techniques[7]. In brief, exosome suspensions were fixed with 2% glutaraldehyde supplemented with 0.15 M sodium cacodylate and post-fixed with 1% OsO_4. They were then dehydrated with ethanol and embedded in Epon 812. Samples were sectioned, post-stained with uranyl acetate and lead citrate, and examined with an electron microscope. For immune-electron microscopy, cells were fixed with a solution of 4% paraformaldehyde, 2% glutaraldehyde and 0.15 M sodium cacodylate and processed as above. Sections were probed with anti-CD63 (Santa Cruz Biotechnology, sc15363) or anti-CD9 (Abcam, ab92726) antibodies (or rabbit IgG as a control) and visualized with immunogold-labelled secondary antibodies. Immuno-electron microscopy analysis revealed that the isolated exosomes were 50–200 nM in diameter and stained positively for the tetraspanin exosome markers CD63 and CD9 (ref. 46).

Exosome number estimation assay. Exosomal concentration was assessed using the EXOCET ELISA assay (System Biosciences), which measured the esterase activity of cholesteryl ester transfer protein (CETP) activity. CETP is known to be enriched in exosomal membranes. The assay was calibrated using a known isolated exosome preparation (System Biosciences). Additionally, exosome preparations were subjected to the qNano system employing tunable resistive pulse sensing technology (IZON technologies) to measure the number and size distribution of exosomes.

Serum miRNA isolation. For total serum miRNA isolation, 100 μl of serum was obtained from ADicerKO mice or Lox littermates and miRNAs were isolated using an Exiqon miRCURY Biofluid RNA isolation kit following the manufacturer's protocol.

RNA isolation and real-time PCR analysis. RNA was isolated from exosomal preparations using TRIzol, following the manufacturer's protocol (Life Sciences). Subsequently, 50 ng of exosomal RNA was subjected to reverse transcription into cDNA by using a mouse miRNome profiler kit (System Biosciences). qPCR was then performed in 6-μl reaction volumes containing cDNA along with universal primers for each miRNA and SYBR Green PCR master mix (Bio-Rad).

Bioinformatics qRT–PCR data analysis. In line with previous research, for all serum and exosomal miRNA quantitative PCR reactions the C_t values were normalized using U6 snRNA as an internal control. To estimate miRNA abundance in fat tissue, data were normalized using the global average of expressed C_t values per sample[47], as the snRNA U6 was differentially expressed between depots. For all quantitative PCR reactions involving gene expression calculations for FGF21, normalization was carried out by using the TATA-binding protein as an internal control. Differential expression analysis of the high-throughput $-\Delta C_t$ values was done using the Bioconductor limma package[48] in R (www.r-project.org). Fold differences in comparisons were expressed as $2^{-\Delta\Delta Ct}$. Ct Principal component analysis plots were created using R with the *ggplot2* package.

Heatmaps of miRNA expression. A detection threshold was set to $C_t = 34$ for all mouse miRNA PCR reactions; no threshold was used for human miRNA PCR, according to the manufacturer's recommendation (System Biosciences). An miRNA was plotted only if its raw C_t value was ≤ 34 in at least three samples, except for the brown pre-adipocyte and 4-week-old mouse experiments, in which the raw C_t only had to be ≤ 34 twice. miRNA $-\Delta C_t$ values were *Z* scored and heatmaps were created by Cluster 3.0 and TreeView programs as previously described[49].

Fat tissue transplantation. Fat tissue transplantation was carried out as previously described[50]. In brief, 10-week-old male Lox donor mice (C57BL/6 males) were killed, and their inguinal, epididymal, and BAT fat depots were isolated, cut into several 20-mg pieces and transplanted into 10-week-old male ADicerKO mice ($n = 5$ male mice per group). Each recipient ADicerKO mice received the equivalent transplanted fat mass of two donor Lox control mice. Transplanted mice received post-surgical analgesic intraperitoneal injections (buprenorphine, 50 mg/kg) for 7 days. At day 12, a glucose tolerance test was performed after a 16-h fast by intraperitoneal injection of 2 g/kg glucose. All mice were killed after 14 days. All procedures were conducted in accordance with Institutional Animal Care and Use Committee regulations.

Luciferase vectors and *in vitro* assays. An adenoviral *Fgf21* 3′ UTR reporter was created by cloning the 3′ UTR of *Fgf21* into the pMir-Report vector. Subsequently, the luciferase-tagged 3′ UTR fragment was cloned into the adenoviral vector pacAd5-CMV-IRES-GFP, creating an adenovirus bearing the *Fgf21* 3′UTR reporter. Hsa-miR-302f-3′-UTR was created by cloning the synthesized Luc-miR-302f-3′-UTR fragment (Genescript) into the Viral Power Adenoviral Expression System (Invitrogen). *In vitro* bioluminescence was measured using a dual luciferase kit (Promega).

***In vivo* regulation of FGF21 experiments.** Eight-week-old male ADicerKO or wild-type mice were injected intravenously with adenovirus bearing the 3′-UTR of *Fgf21* fused to the luciferase gene to create two groups of liver-reporter mice—one with a ADicerKO background and one with a wild-type background. One day later, a third group of ADicerKO mice, which had also been injected intravenously with an adenovirus bearing the 3′-UTR of *Fgf21* fused to the luciferase gene, were injected intravenously with exosomes isolated from the serum of wild-type mice. After 24 h, *in vivo* luminescence of the *Fgf21* 3′ UTR was measured using the IVIS imaging system (Perkin Elmer) by administering D-luciferin (20 mg/kg) according to the manufacturer's protocol (Perkin Elmer).

For the second group, 8-week-old male ADicerKO or wild-type mice were also transfected with adenovirus bearing the 3′ UTR of *Fgf21* fused to the luciferase gene by intravenous injection. After 1 day, mice received an intravenous injection of exosomes isolated from the serum of either ADicerKO mice or ADicerKO mice reconstituted *in vitro* with 10 nM miR-99b by electroporation. Twenty-four hours later, *in vivo* luminescence was measured using the IVIS imaging system by administering D-luciferin (20 mg/kg) according to the manufacturer's protocol (Perkin Elmer).

BAT-derived exosomes expressing human miRNA targeting the liver. *Protocol 1.* On day 0, adenovirus bearing either pre-hsa_miR-302f or *lacZ* mRNA (as a control) was injected directly into the BAT of 8-week-old male C57BL/6 mice. Hsa_miR-302f is human-specific and does not have a mouse homologue. This procedure was conducted under ketamine-induced anaesthesia. Four days later, the same mice were injected intravenously with an adenovirus bearing the 3′ UTR of miR-302f in-frame with the luciferase gene, thereby transducing the liver tissue of the mouse with this human 3′ UTR miRNA reporter. Suppression of the 3′ UTR miR-302f reporter would occur only if there was communication between the BAT-produced miRNA and the liver. *In vivo* luminescence was measured on day 6 using the IVIS imaging system as described above.

Protocol 2. To assess specifically the role of exosomal miR-302f in the regulation of its target reporter in the liver, two separate cohorts of 8-week-old male C57BL/6 mice were generated. One cohort was injected with adenovirus bearing pre-miR-302f or *lacZ* directly into the BAT (the donor cohort); the second cohort was transfected with an adenovirus bearing the 3′ UTR reporter of this miR-302f in the liver, as described for Protocol 1 (the acceptor cohort). Serum was obtained on days 3 and 6 from the donor cohorts; the exosomes were isolated and then injected intravenously into the acceptor mice the next day (days 4 and 7). On day 8, *in vivo* luminescence was measured in the acceptor mice using the IVIS imaging system as described above.

Adenoviral DNA isolation. To test for the presence of adenovirus in the liver and BAT of C57BL/6 mice, 100 mg tissue was homogenized in 1 ml sterile 1× PBS. The homogenate was spun down and 150 μl cleared supernatant was used to isolate adenoviral DNA using the Nucleospin RNA and DNA Virus kit, following the manufacturer's protocol (Takara). PCR was performed on 2 μl isolated adenoviral DNA using SYBR green to detect *lacZ* or miR-302f amplicons.

qRT–PCR fat tissue transplantation analysis. For all PCR data obtained in the fat-tissue-transplantation experiment, an miRNA was considered to be present

only if its mean C_t in the wild-type group was <34. We then identified those miRNAs that were significantly decreased in ADicerKO serum. For an miRNA to be considered restored after transplantation by a particular depot it had to be significantly increased from ADicerKO serum with a mean $C_t < 34$ and its C_t had to be more than 50% of the way from ADicerKO to the wild type on the C_t scale.

Statistical analysis. ANOVA tests were followed by two-tailed Dunn's post-hoc analysis or Tukey's multiple comparisons test to identify statistically significant comparisons. All *t*-tests and Mann–Whitney *U*-tests were two-tailed. *P* values less than 0.05 were considered significant. All ANOVA, *t*-tests, and area-under-the-curve calculations were carried out in GraphPad Prism 5.0.

miRDB analysis. For miRDB analysis (http://www.mirdb.org), a search by target gene was performed against the mouse database. A target score of 85 was set to exclude potential false-positive interacting miRNAs.

Data and code availability. All high-throughput qRT–PCR data (raw C_t values), the code used to analyse them (in the free statistical software R), and its output (including supplementary tables, tables used to generate heatmaps, and statements in the text) can be freely downloaded and reproduced from https://github.com/jdreyf/fat-exosome-microrna. All other data are available from the corresponding author upon reasonable request.

45. Tian, Y. *et al.* A doxorubicin delivery platform using engineered natural membrane vesicle exosomes for targeted tumor therapy. *Biomaterials* **35,** 2383–2390 (2014).
46. Mathivanan, S., Fahner, C. J., Reid, G. E. & Simpson, R. J. ExoCarta 2012: database of exosomal proteins, RNA and lipids. *Nucleic Acids Res.* **40,** D1241–D1244 (2012).
47. Mestdagh, P. *et al.* A novel and universal method for microRNA RT–qPCR data normalization. *Genome Biol.* **10,** R64 (2009).
48. Smyth, G. K. Linear models and empirical bayes methods for assessing differential expression in microarray experiments. *Stat. Appl. Genet. Mol. Biol.* **3,** Article3 (2004).
49. Eisen, M. B., Spellman, P. T., Brown, P. O. & Botstein, D. Cluster analysis and display of genome-wide expression patterns. *Proc. Natl Acad. Sci. USA* **95,** 14863–14868 (1998).
50. Tran, T. T., Yamamoto, Y., Gesta, S. & Kahn, C. R. Beneficial effects of subcutaneous fat transplantation on metabolism. *Cell Metab.* **7,** 410–420 (2008).

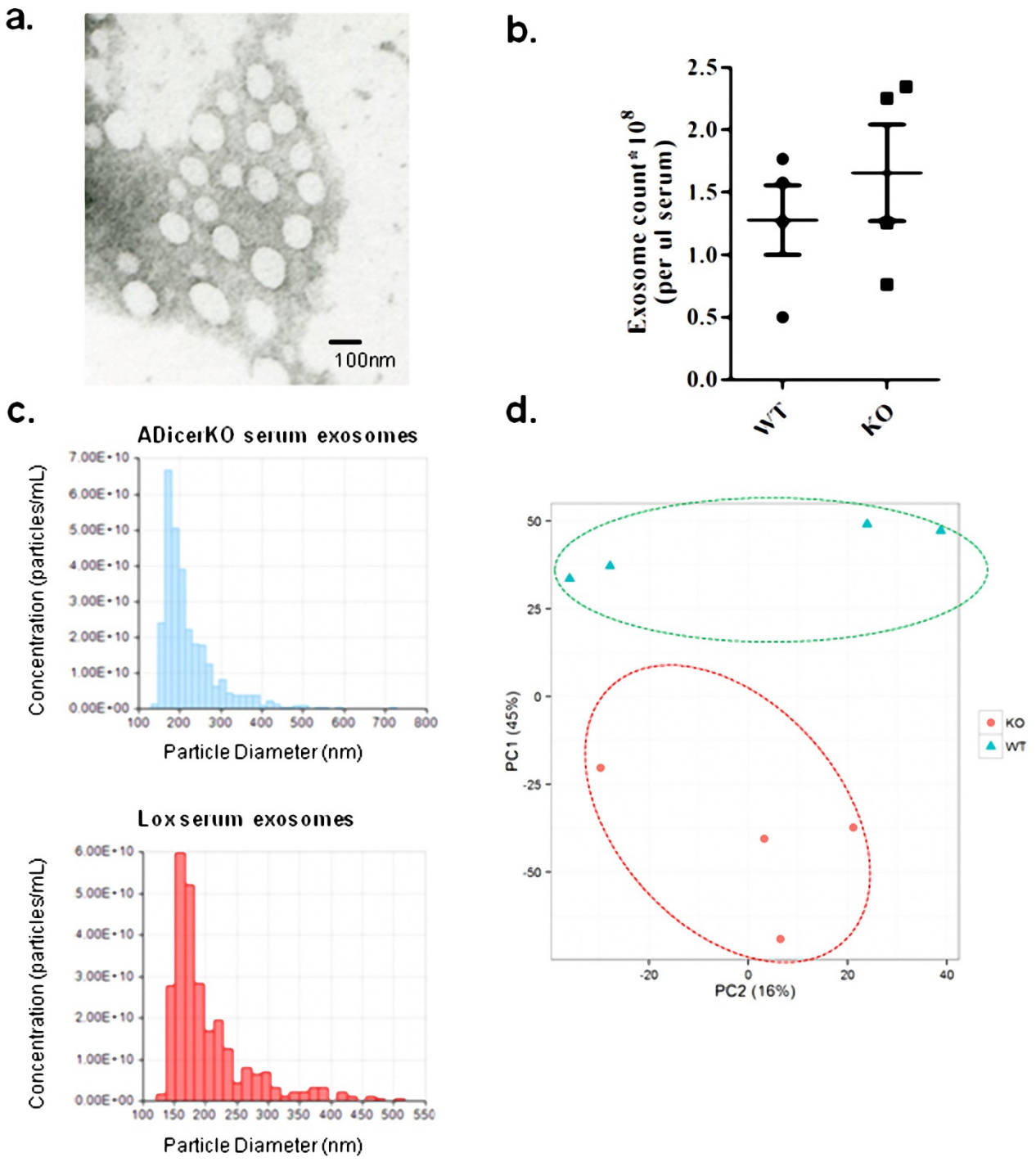

Extended Data Figure 1 | Fat is a major source of circulating exosomal miRNAs in mice. a, Electron micrograph of exosomes isolated from ADicerKO serum by differential centrifugation. **b**, EXOCET ELISA assay measuring CETP protein in exosome samples, corresponding to isolated exosome number from serum of ADicerKO (KO) or Lox (WT) mice. **c**, qNano assay measuring the number and size of exosomes, based on tunable resistive pulse sensing technology from exosome preparations from ADicerKO (top) or Lox (bottom) mice. **d**, Principle component analysis of exosomal miRNA levels in ADicerKO and Lox mice, $n = 4$ per group. Data are mean s.e.m.

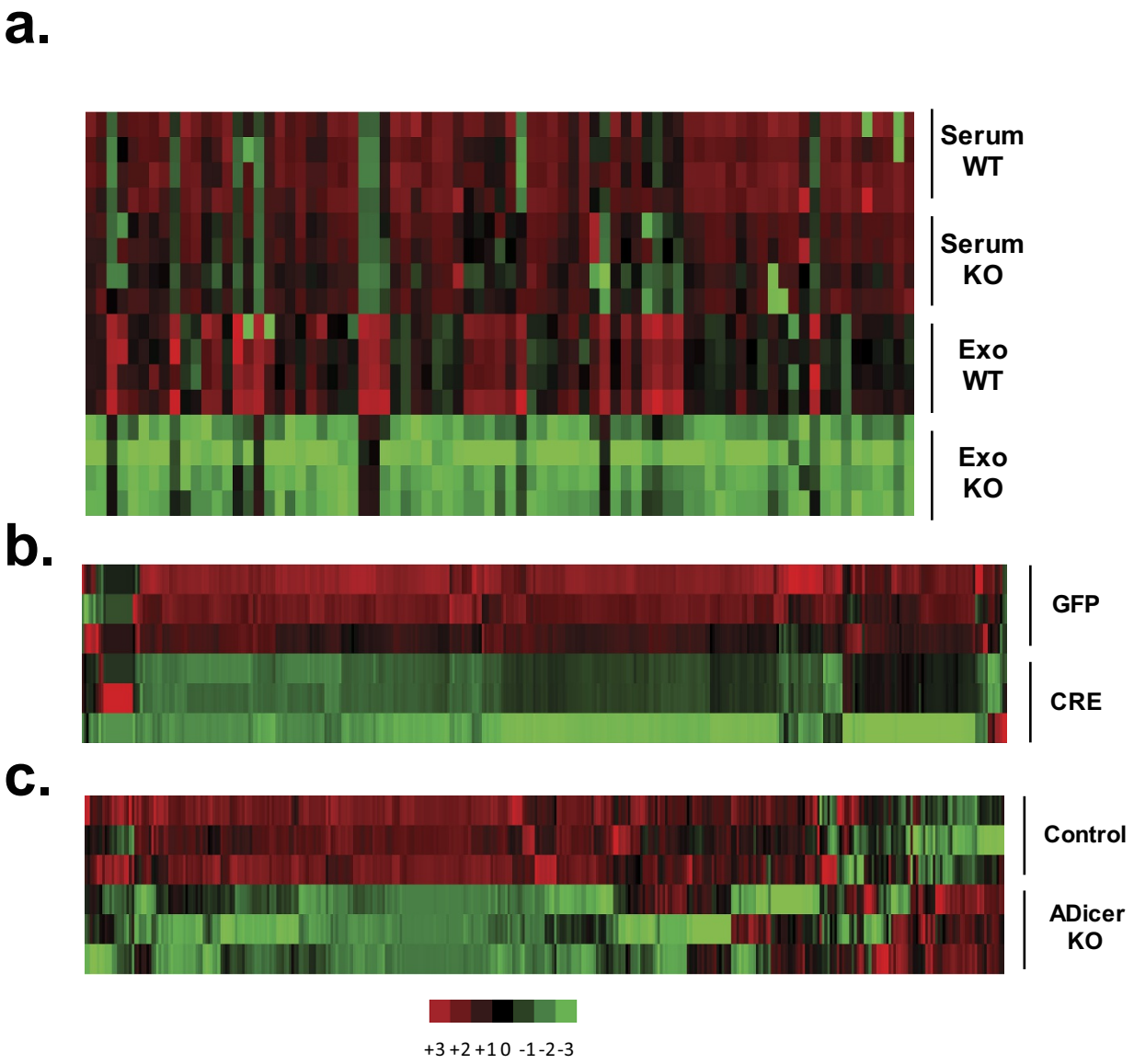

Extended Data Figure 2 | Adipose tissue Dicer regulates exosomal and serum miRNA content. a, Heatmap showing *Z* scores of miRNA expression in whole serum from ADicerKO (KO) and wild-type mice (WT), and exosomal miRNAs from ADicerKO (ExoKO) or wild-type mice (ExoWT) ($n = 4$ per group). **b**, Heatmap showing *Z* scores of expression of exosomal miRNAs from culture supernatant of $Dicer^{fl/fl}$ pre-adipocytes transfected with adenovirus encoding GFP or Cre ($n = 3$ per group). **c**, Heatmap showing *Z* scores of miRNA expression measurements of exosomal miRNAs from the serum of 4-week-old ADicerKO (AdicerKO) and Lox (Control) mice ($n = 3$ per group).

a.

Features	Controls	HIV Lipodystrophy
N	4	4
Age	52 ± 2	53± 3
BMI	27 ± 1	26 ± 1
Weight	75 ± 4	67 ± 7
CD4 cell count	N/A	414 ± 142
Duration HIV (yrs)	N/A	18 ± 1.9
Serum chol. (mg/dL)	185 ± 8	180 ± 15

Features	Controls	Lipo dystrophy
N	4	4
Age	52 ± 2	13 ± 4
BMI	27 ± 1	17.7 ± 2.1
Serum cholesterol (mg/dL)	185 ± 8	233 ± 20

b.

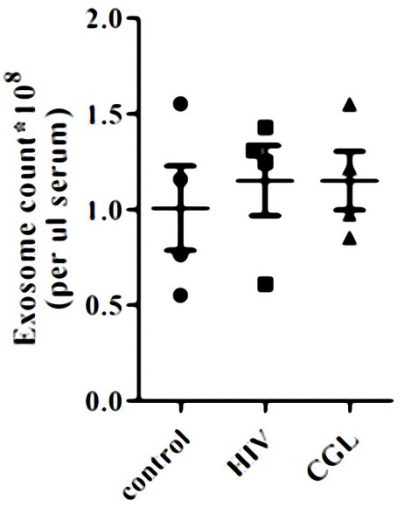

c.

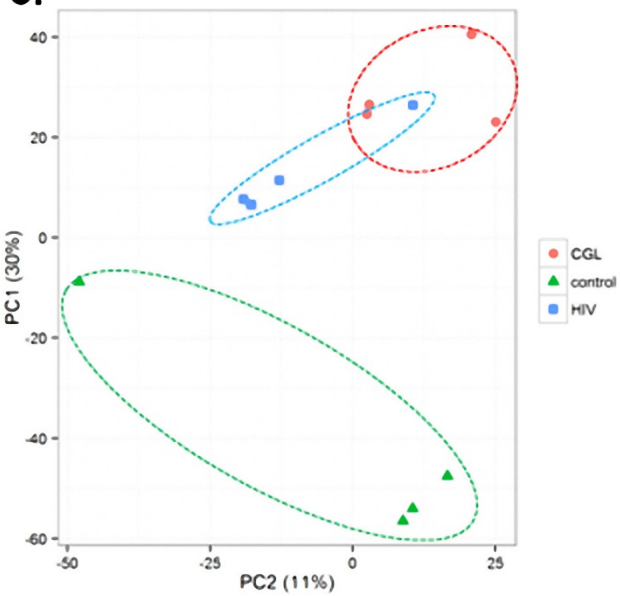

Extended Data Figure 3 | Fat is a major source of circulating exosomal miRNAs in humans. a, Demographic information about human patients with HIV-associated lipodystrophy, CGL (labelled as Lipodystrophy) or control subjects. **b**, EXOCET ELISA assay measuring CETP protein as a measure of exosome number from isolated from human sera of individuals with HIV-associated lipodystrophy (HIV), CGL and control subjects ($n = 4$ per group). **c**, Principle component analysis of exosomal miRNA expression in patients with HIV-associated lipodystrophy or CGL, or in control subjects ($n = 4$ per group). Data are mean ± s.e.m.

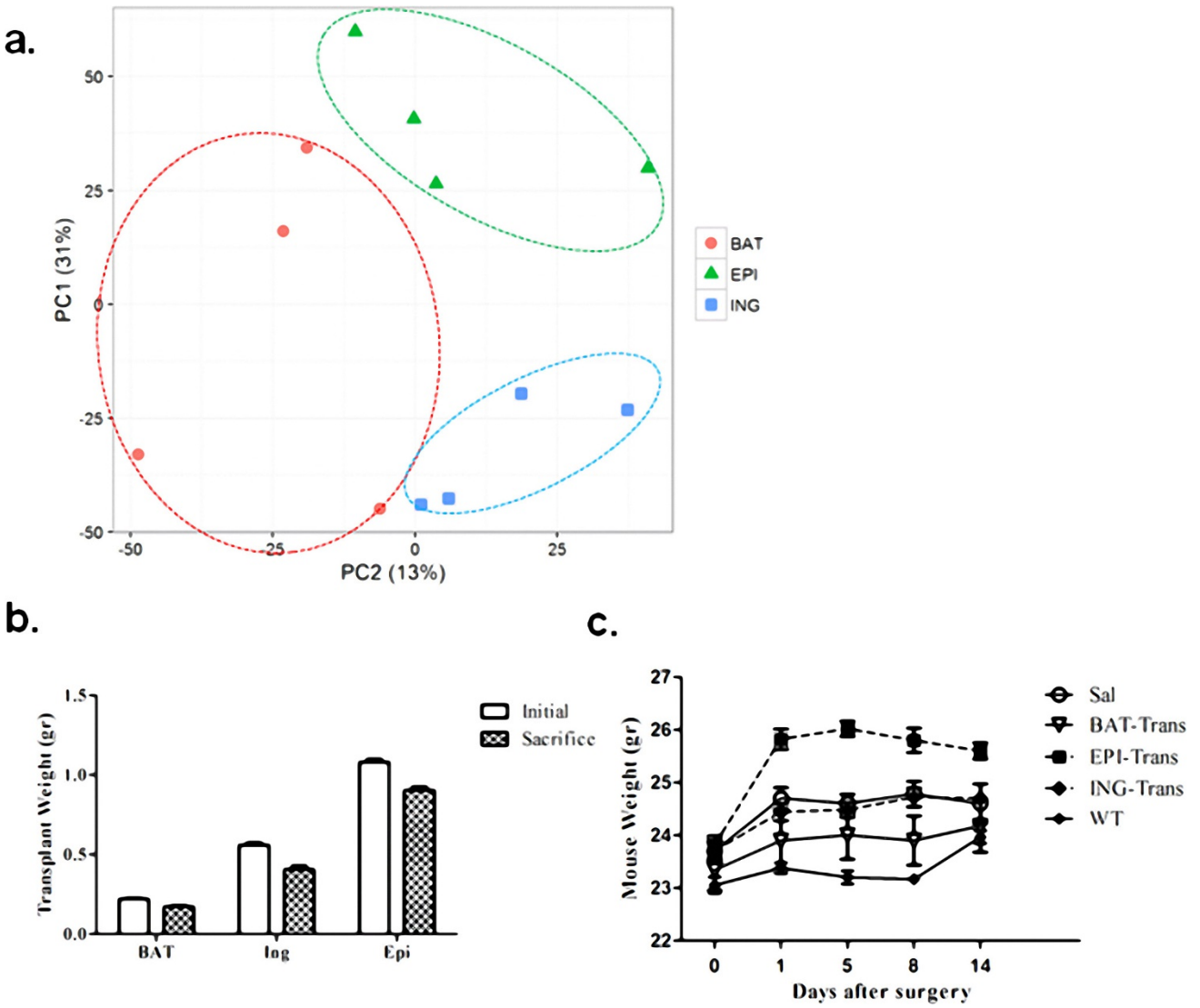

Extended Data Figure 4 | Transplant donor fat depot miRNA signatures are distinct. a, Principle component analysis of miRNA expression in mouse epididymal (EPI), inguinal (ING) and BAT fat depots ($n = 4$ per group). **b**, Weight of the transplanted epididymal WAT, inguinal WAT and BAT at time of transplantation into ADicerKO mice (white bars) and at time of death (chequered bars) ($n = 3$). **c**, Weight of ADicerKO mice that underwent sham surgery (Sal) or transplantation with epididymal, inguinal, or BAT fat; Lox mice that underwent sham surgery (WT) serve as a control. Data are mean ± s.e.m.

a.

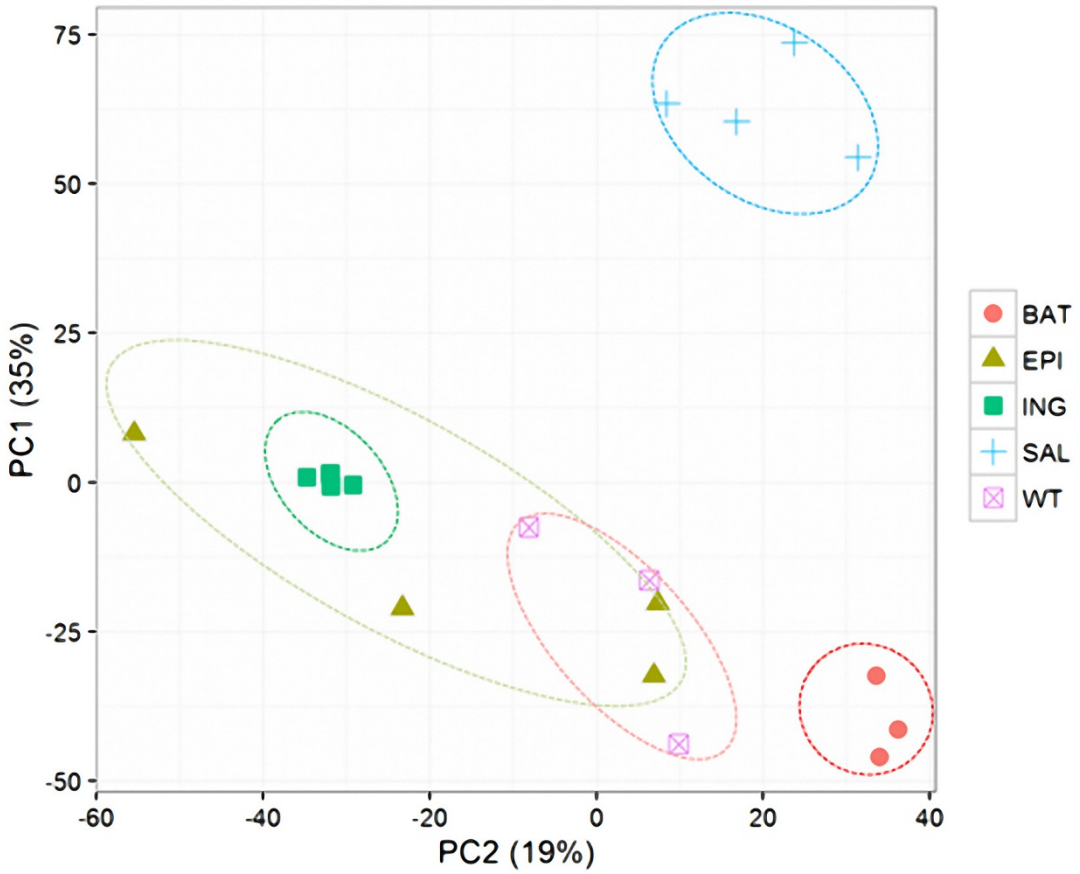

b.

	WT	KO			
		SAL	EPI	ING	BAT
INSULIN (pg/ml)	136 ± 53	451 ± 169	631 ± 264	589 ± 283	332 ± 62
IL-6 (pg/ml)	11.3 ± 2.6	7.8 ± 2.3	6.9 ± 0.6	5.8 ± 1.6	6.7 ± 1.1
LEPTIN (pg/ml)	4764 ± 1678	3573 ± 929	4750 ± 2091	4578 ± 1087	4080 ± 743
ADIPONECTIN (pg/ml)	0.74 ± 0.18	0.3 ± 0.08	0.33 ± 0.11	0.61 ± 0.14	0.48 ± 0.04

Extended Data Figure 5 | Fat tissue transplantation alters exosomal miRNA content. a, Principle component analysis of serum exosomal miRNA levels in ADicerKO mice after sham surgery (Sal) or transplantation with inguinal fat (ING), epididymal fat (EPI) or BAT; Lox littermates that underwent sham surgery serve as a control ($n = 4$ per group). **b**, Circulating levels of insulin and the adipokines IL-6, leptin and adiponectin in the groups of mice in **a**. Two-tailed t-test, $P < 0.05$ ($n = 3$ per group).

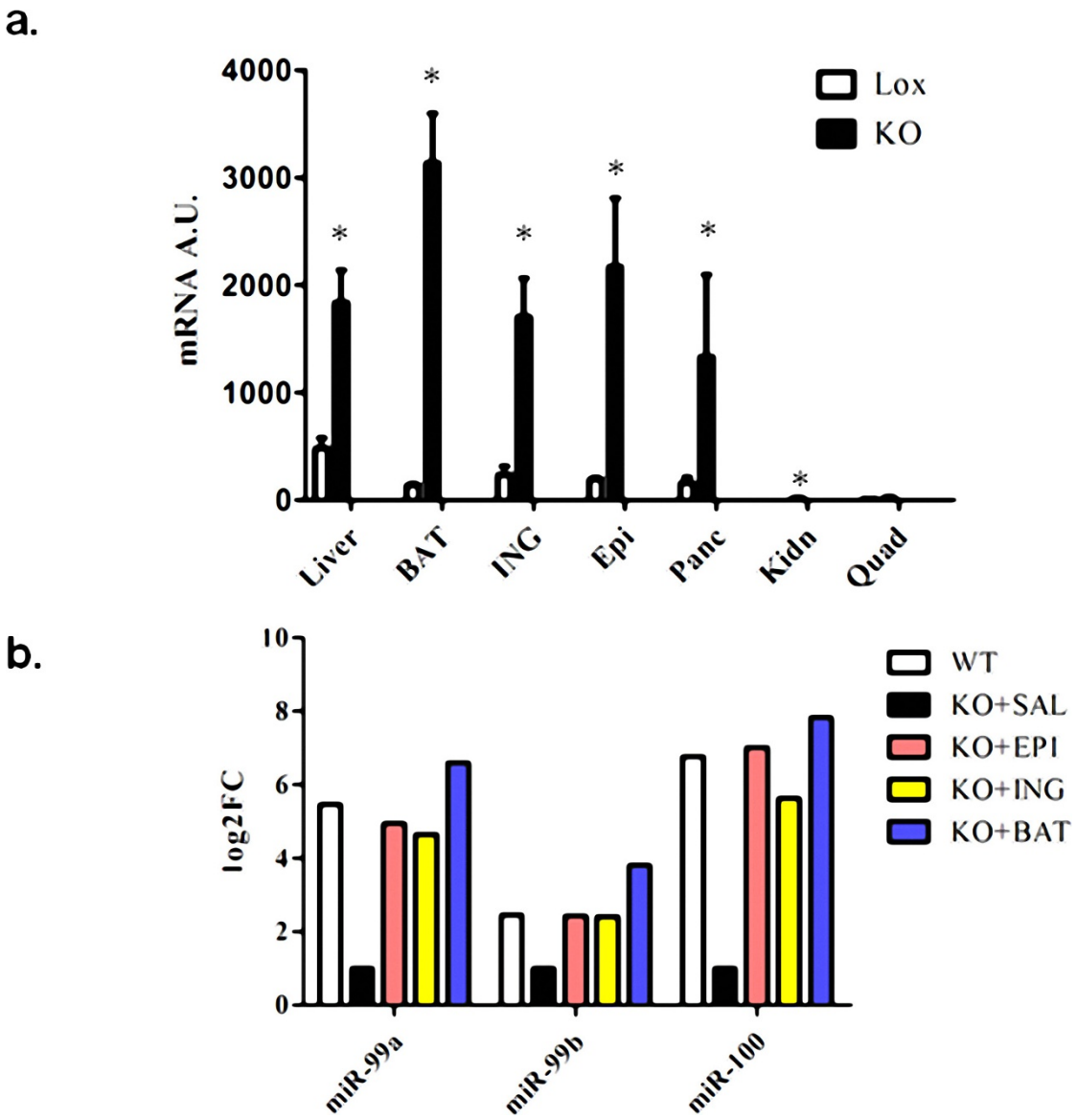

Extended Data Figure 6 | ADicerKO mice exhibit reduced *Fgf21* abundance. a, Levels of *Fgf21* mRNA, as assessed by qRT–PCR in liver, BAT, inguinal (ING), epididymal (Epi), pancreas (Panc), kidney (Kidn) and quadriceps muscle (Quad) tissue from ADicerKO mice (black bars) or Lox littermates (white bars). $P = 0.0286$ by two-tailed Mann–Whitney U test ($n = 4$ per group)**. b**, Relative abundance (shown as $\log_2$ fold change (log2FC)) as assessed by qRT–PCR of miR-99a, miR-99b, and miR-100 in exosomes extracted from ADicerKO (KO) mice that underwent sham or fat-transplantation surgery (as in Fig. 2e) and wild-type mice that underwent sham surgery ($n = 4$ per group). Data are mean ± s.e.m. *$P = 0.05$.

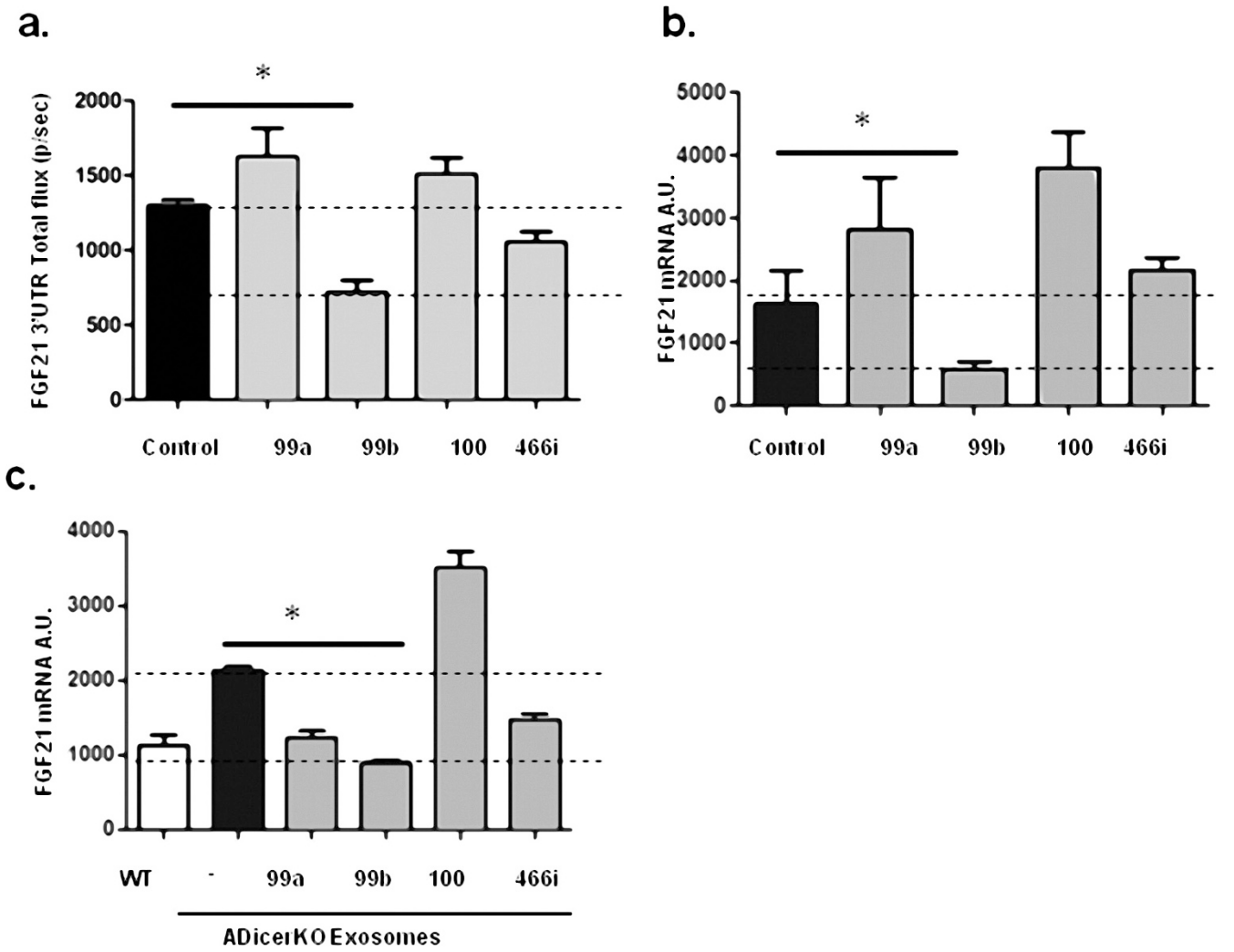

Extended Data Figure 7 | *Fgf21* is regulated by exosomal fat-derived miRNAs *in vitro*. **a**, *Fgf21* 3′ UTR luciferase-reporter activity in AML-12 mouse liver cells after transfection with 10 nM miR-99a, miR-99b, miR-100, miR-466i or control by direct electroporation. $P = 0.003$ by two-tailed *t*-test ($n = 3$ per group). **b**, Abundance of *Fgf21* mRNA in AML-12 mouse liver cells following transfection with 10 nM miRNA miR-99a, miR-99b, miR-100 or miR-466i. $P = 0.037$, two tailed *t*-test ($n = 3$ per group). **c**, Hepatic *Fgf21* mRNA levels by qRT–PCR followed by a 48-h incubation of AML-12 hepatic cells with exosomes derived from Lox or ADicerKO (−) mice, or with exosomes from ADicerKO mice electroporated with 10 nM miR-99a, miR-99b, miR-100 or miR-466i. $P = 0.0001$, two-tailed *t*-test ($n = 3$ per group). Data are mean ± s.e.m. *$P = 0.05$.

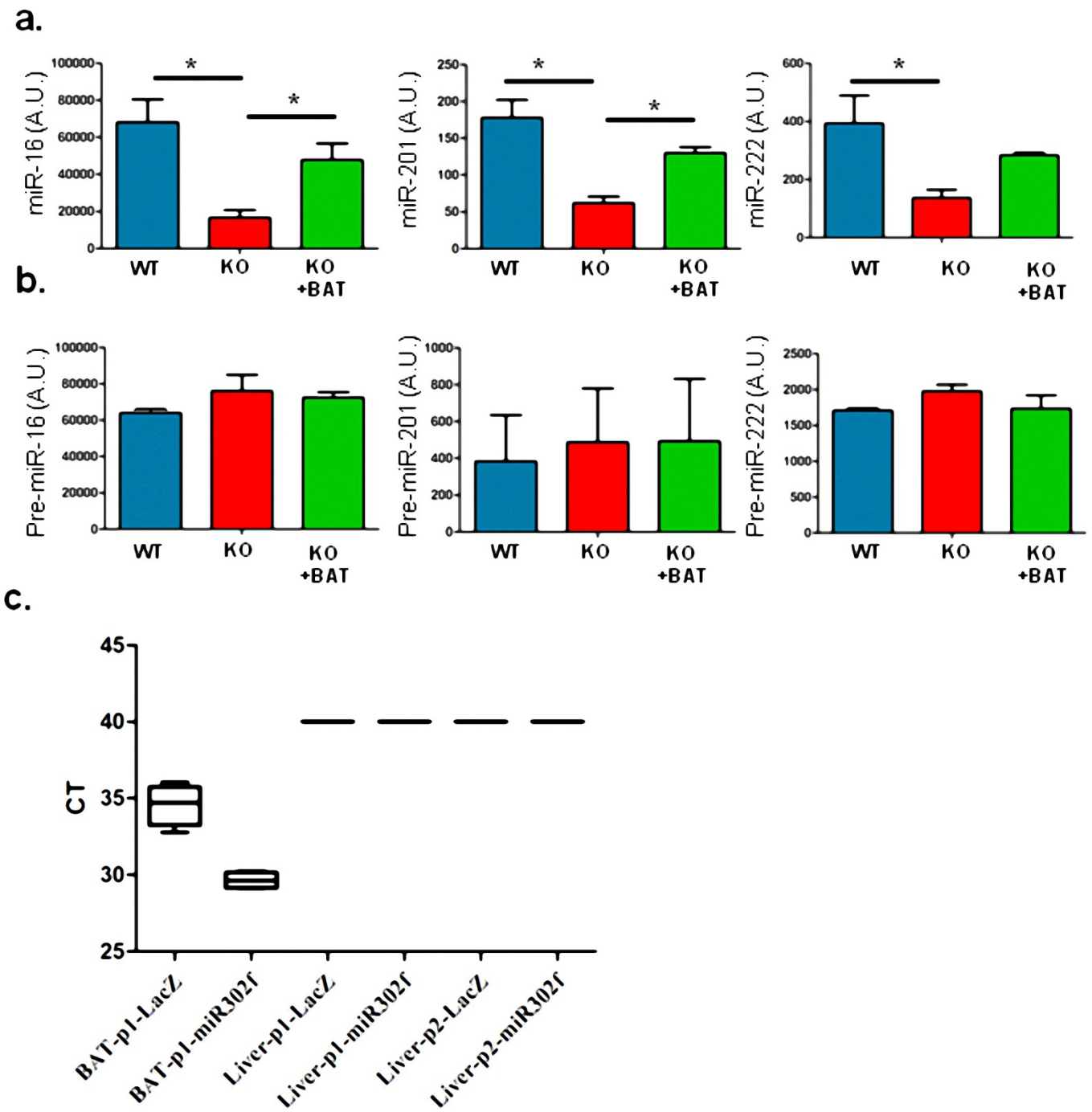

Extended Data Figure 8 | Adipose tissue-specific miRNAs are enriched in the liver after fat transplantation. a, qRT–PCR quantification of levels of mature miR-16, miR-201, and miR-222 in liver from Lox mice, ADicerKO mice and ADicerKO mice transplanted with BAT (KO + BAT). $P = 0.02$ for miR-16, $P = 0.002$ for miR-201, and $P = 0.028$ for miR-222; one-way ANOVA; significant comparisons were identified by Tukey's multiple comparisons test ($n = 3$ per group). **b**, qRT–PCR quantification of the levels of pre-miR-16, pre-miR-201, and pre-miR-222 in the livers of Lox mice, ADicerKO mice and ADicerKO mice transplanted with BAT. $P < 0.05$, one-way ANOVA ($n = 3$ per group,). **c**, qRT–PCR-derived C_t values of adenoviral DNA isolated from BAT and liver tissue in Protocol 1 (BAT-p1 and Liver-p1, respectively), and from liver tissue in Protocol 2 (liver-p2), detecting adenoviral *lacZ* or pre-miR-302f ($n = 4$ per group). Data are mean ± s.e.m. *$P = 0.05$.

CORRECTIONS & AMENDMENTS

CORRIGENDUM

doi:10.1038/nature22319

Corrigendum: Adipose-derived circulating miRNAs regulate gene expression in other tissues

Thomas Thomou, Marcelo A. Mori, Jonathan M. Dreyfuss, Masahiro Konishi, Masaji Sakaguchi, Christian Wolfrum, Tata Nageswara Rao, Jonathon N. Winnay, Ruben Garcia-Martin, Steven K. Grinspoon, Phillip Gorden & C. Ronald Kahn

Nature **542,** 450–455 (2017); doi:10.1038/nature21365

In this Article, in Fig. 4f–h, the *x*-axis labels 'WT + exoKO' and 'ADicerKO + exoKO' were inadvertently reversed, and in Fig. 5c, f, the *y*-axis labels should have been labelled 'miR-302f 3′UTR total flux' rather than '*Fgf21* 3′UTR total flux'. In Fig. 4b and f, the units for the *y*-axis labels should have been listed as '(photons s^{-1})' instead of '(photons $s^{-1} \times 10^{10}$)'. The data in all panels remain unchanged, and these errors do not affect the results or conclusions of the Article. We apologize for these errors. In addition, the following sentence has been added to the Fig. 4 legend for added clarity: "Note that the order of the data in **f**–**h** is different from the order of the mice shown in **e** because the IVIS scan was done in a blinded fashion." The original Article has been corrected online.